

On the Fermion Sign Problem in Imaginary-Time Projection Continuum Quantum Monte Carlo with Local Interaction

Francesco Calcapecchia*

LPMMC, UMR 5493, Boîte Postale 166, 38042 Grenoble, France

Institute of Physics, Johannes Gutenberg-University, Staudingerweg 7, D-55128 Mainz, Germany and Graduate School of Excellence Materials Science in Mainz, Staudingerweg 9, D-55128 Mainz, Germany

Markus Holzmann†

LPMMC, UMR 5493 of CNRS, Université Grenoble Alpes, 38042 Grenoble, France and

Institut Laue Langevin, BP 156, F-38042 Grenoble Cedex 9, France

We use the Shadow Wave Function formalism as a convenient model to study the fermion sign problem affecting all projector Quantum Monte Carlo methods in continuum space. We demonstrate that the efficiency of imaginary time projection algorithms decays exponentially with increasing number of particles and/or imaginary-time propagation. Moreover, we derive an analytical expression that connects the localization of the system with the magnitude of the sign problem, illustrating this prediction through some numerical results. Finally, we discuss the fermion sign problem computational complexity and methods for alleviating its severity.

INTRODUCTION

The *fermion sign problem* is one of the most renowned open problems in computational physics. It consists into finding a general algorithm able to determine the exact fermionic ground state with a computational cost that grows polynomially with the number of simulated particles. In fact, all the known exact algorithms for classical computers scale exponentially except for a small class of model systems [1–3]. In particular, Quantum Monte Carlo (QMC) methods [4–7], which are able to provide the exact *bosonic* ground state in polynomial time for a wide range of Hamiltonians, suffer from a sign problem when applied to fermions. In the following we will often refer to the solution of the fermion sign problem, implicitly meaning that the exact fermion ground state is obtained in polynomial time rather than in exponential time in respect to the number of particles.

What is especially remarkable about the fermion sign problem in QMC is that, despite various attempts within all kind of flavours, it still remains unsolved. This is a reminiscence of the Non-deterministic Polynomial Complete (NPC) problems, a set of hundreds of apparently different problems that, despite many efforts, have not been solved yet. The most famous of such problems is the Travelling Salesman, formulated in 1930. Notably, it has been found that all these problems are mappable one into the other, so that the solution of one of them would imply the solution of all of them [8]. The fact that it has not been possible to solve not even one of them, justifies the common belief that these problem are intractable. As a matter of fact, NPC problems are so firmly believed to be intractable, that all the classical encryption schemes rely on this conjecture. However, despite the importance

of this conjecture (known in the literature as $NP \neq P$ hypothesis), a proof is still missing.

In 2005 Troyer and Wiese provided a demonstration of the NP-hardness of the Monte Carlo (MC) sign problem [9] for a specific Hamiltonian. The NP-hard problems are a class of problems which are mappable in polynomial time into NPC so that solving any NP-hard problem would provide the solution to all the NPC problems. In this sense NP-hard problems are said to be the hardest ones, as they are at least as hard as any other NPC problem.

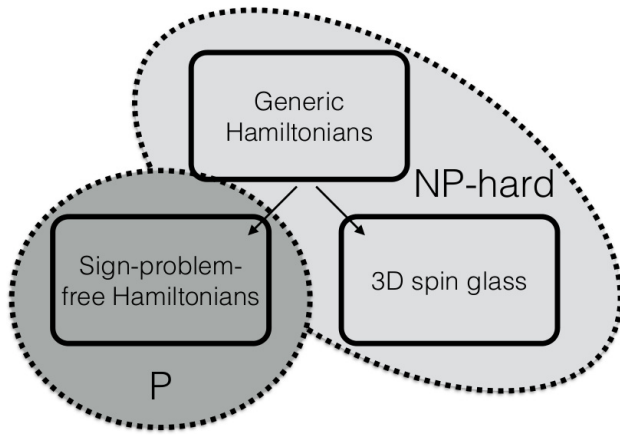


Figure 1. Diagram of the up-to-date scenario of QMC simulation computational complexity.

In the present paper, we focus on the class of fermionic QMC simulations of continuum systems with local interactions, e.g. non-relativistic electrons interacting via static Coulomb potential, and try to understand as much as possible about the corresponding fermion sign problem. In particular, we study the performance of the imaginary-time projection techniques, which provide polynomial scaling solutions to the corresponding bosonic

* francesco.calcapecchia@gmail.com

† markus.holzmann@grenoble.cnrs.fr

problems. Our discussion is based on the Shadow Wave Function (SWF) formalism [10]. If the fermion sign problem can be solved for the SWF, such solution will be extendable to all the other QMC methods. Whereas, if SWF proved to fall in the NP-hard class, the same applies to the other imaginary-time projections QMC methods.

We remark that, even if a problem is NP-hard, one can obtain approximate solutions, and work on the improvement of the approximations. For example, even though the Traveller Salesman problem cannot be solved exactly for many problems of practical interest, there are several approximated methods that are able to provide excellent solutions [12, 13]. Similarly, concerning the fermion sign problem, there have been remarkable progress over the recent years obtained by employing more flexible trial wave functions and improved of optimization procedures, which permit to systematically reduce the deviation from the exact ground state [14–17].

A different strategy which we study in this paper is to alleviate the sign problem, where, similar to the released-node algorithm [18] and different exact fermion simulations [19–25], one aims to reduce the pre-factor of the ultimate exponential decay in the signal of the desired quantities. In the following, we refer to the Monte Carlo *efficiency*, defined as

$$\eta \equiv \frac{1}{\text{cpu time} \times \text{var}}, \quad (1)$$

where *var* is the variance of the computed quantity. The SWF is a perfect tool-bench for a systematic study of the efficiency of different strategies, as the severity of the sign problem can be controlled by kernel parameters, and the method itself is considerably cheaper than most of imaginary-time projection methods.

This paper is structured as follows. In Sec. I we introduce the Shadow Wave Function formalism, and then explain its connection with Diffusion Monte Carlo and Path Integral Ground State in Sec. II. We will characterize its fermion sign problem when using a Slater determinant of simple plane waves in Sec. III, and generalize this result to orbitals of any kind in Sec. IV. We will then review some general method that have been proposed to tackle the fermion sign problem in Sec. V, and finally discuss about its computational complexity in Sec. VI. The conclusion are drawn in Sec. VII.

I. THE SHADOW WAVE FUNCTION FORMULATION

The Shadow Wave Function (SWF) is a class of variational trial wave functions which, by embedding an integral, can profit from a great flexibility [10, 11]. In general, the SWF can be written as

$$\begin{aligned} \Psi_{\text{SWF}}(R) &= J_{\text{R}}(R) \int dS \Xi(R, S) \varphi_{\text{T}}(S) \\ &= \int dS \varphi_{\text{SWF}}(R, S) \end{aligned} \quad (2)$$

where $R \equiv (\mathbf{r}_1, \mathbf{r}_2, \dots, \mathbf{r}_N)$ represents the particle coordinates, S labels some $3N$ -dimensional auxiliary coordinates, J_{R} is a Jastrow, φ_{T} is a chosen trial wave function, and

$$\Xi(R, S) = e^{-C(R-S)^2} \quad (3)$$

is the so-called *kernel*. The SWF efficiently removes large part of the bias introduced by the underlying trial wave function, in particular close to phase transitions or in inhomogeneous systems [26–31].

The application of the SWF to fermions requires the fulfilment of the Fermi-Dirac statistics by the use of an antisymmetric form for spin-like particles. In the following we split the trial wave function into the product of a symmetrical part, the Jastrow factor, times an antisymmetrical part, usually taken as a Slater determinant.

A straightforward antisymmetrization of Eq. (2) gives the Fermionic Shadow Wave Function (FSWF) form

$$\begin{aligned} \Psi_{\text{FSWF}}(R) &= J_{\text{R}}(R) \int dS \Xi(R, S) J_{\text{S}}(S) \Phi(S) \\ &= \int dS \varphi_{\text{FSWF}}(R, S) \end{aligned} \quad (4)$$

where Φ represents a Slater determinant and J_{S} a Jastrow. Unfortunately, the FSWF introduces a sign problem [32] which emerges by the fact that the product $\varphi_{\text{FSWF}}^*(R, S_1) \times \varphi_{\text{FSWF}}(R, S_2)$ is not necessarily positive.

The sign problem of FSWF is avoided using the Antisymmetric Shadow Wave Function (ASWF)

$$\begin{aligned} \Psi_{\text{ASWF}}(R) &= J_{\text{R}}(R) \Phi(R) \int dS \Xi(R, S) J_{\text{S}}(S) \\ &= \int dS \varphi_{\text{ASWF}}(R, S), \end{aligned} \quad (5)$$

since $\varphi_{\text{ASWF}}^*(R, S_1) \times \varphi_{\text{ASWF}}(R, S_2)$ is garantied to be positive for any R , S_1 and S_2 .

Typically, FSWF is considered of higher quality and is expected to lead to a lower variational energy than ASWF.

II. CONNECTION BETWEEN SWF, DMC, AND PIGS

The SWF can be regarded as a prototype method for any kind of imaginary-time projection method, since the kernel has the form of an approximated Green function with C proportional to the inverse imaginary-time propagation τ .

Consider any trial wave-function φ_{T} not orthogonal to the exact ground state. It is well-known that a propagation in imaginary time will eventually project it to the exact ground state, i.e.

$$e^{-\tau H} |\Psi_{\text{T}}\rangle \xrightarrow{\tau \rightarrow \infty} |\Psi_{\text{GS}}\rangle \quad (6)$$

In order to build a concrete algorithm built upon such property, we make use of the Suzuki-Trotter formula and write

$$e^{-\tau(T+V)} \simeq e^{-\tau T} e^{-\tau V}, \quad (7)$$

which is exact in the limit $\tau \rightarrow 0$.

In order to conciliate the necessity of having a large τ (Eq. (6)) with the Suzuki-Trotter approximation which requires a small τ , we can break the propagation into several small ones. Given a $N_\tau > 1$ such that that $\delta\tau \equiv \tau/N_\tau$ is small enough for the approximation in Eq. (7), the operators $e^{-\delta\tau T} e^{-\delta\tau V}$ can be applied iteratively to the trial wave function to project out the ground state wave function

$$\begin{aligned} |\Psi_{\text{GS}}\rangle &\simeq |\Psi_{\text{T}}[\tau]\rangle \equiv e^{-\tau H} |\Psi_{\text{T}}[0]\rangle \\ &\simeq \left(\prod_{i=1}^{N_\tau} e^{-\delta\tau T} e^{-\delta\tau V} \right) |\Psi_{\text{T}}[0]\rangle \end{aligned} \quad (8)$$

The SWF has the functional form of single propagation $\delta\tau$, since the kinetic energy propagator is a diffusor term in the coordinate space, i.e.

$$\langle R | e^{-\delta\tau T} | R' \rangle \propto e^{-\frac{(R'-R)^2}{4\delta\tau}} \quad (9)$$

Using a variation of the Suzuki-Trotter approximation which splits the potential propagator on the left and on the right symmetrically

$$e^{-\delta\tau(T+V)} \simeq e^{-\frac{\delta\tau}{2}V} e^{-\tau T} e^{-\frac{\delta\tau}{2}V}, \quad (10)$$

we can write (assuming that the potential V is real and local)

$$\begin{aligned} \varphi_{\text{T}}[\delta\tau](R) &= \langle \Psi_{\text{T}}[\delta\tau] | R \rangle \\ &= \langle \Psi_{\text{T}}[0] | e^{-\frac{\delta\tau}{2}V} e^{-\delta\tau T} e^{-\frac{\delta\tau}{2}V} | R \rangle \\ &= \int dS \langle \Psi_{\text{T}}[0] | S \rangle \langle S | e^{-\frac{\delta\tau}{2}V} e^{-\delta\tau T} e^{-\frac{\delta\tau}{2}V} | R \rangle \\ &= \int dS \varphi_{\text{T}}(S) e^{-\frac{\delta\tau}{2}V(S)} e^{-\frac{(R-S)^2}{4\delta\tau}} e^{-\frac{\delta\tau}{2}V(R)} \end{aligned} \quad (11)$$

The generic form of the SWF (Eq. (2)) is the one obtained by mapping

$$\begin{cases} \frac{1}{4\delta\tau} \mapsto C \\ \varphi_{\text{T}}(S) e^{-\frac{\delta\tau}{2}V(S)} \mapsto \varphi_{\text{T}}(S) \\ e^{-\frac{\delta\tau}{2}V(R)} \mapsto J_{\text{R}}(R) \end{cases} \quad (12)$$

In contrast to projector Monte Carlo methods, e.g. Diffusion Monte Carlo (DMC) or Path Integral Ground State Monte Carlo (PIGS), SWF is one step of a chain of small imaginary-time propagations. As a consequence, the SWF cannot expect to be exact, even though it is able to capture most of the corrections provided by the imaginary-time propagation, while retaining a low-computational cost. Further, SWF remains a explicit

trial wave function subject to the Rayleigh-Ritz variational principle, and $\delta\tau$ (corresponding to C) can be regarded as a variational parameter at variance to projector Monte Carlo methods which must be extrapolated to the limit $\delta\tau \rightarrow 0$.

III. THE SIGN PROBLEM OF THE FERMIONIC SHADOW WAVE FUNCTION

The sign problem of the Fermionic Shadow Wave Function has been explored numerically in Ref. [32]. In this section we are going to introduce two different approaches which justify qualitatively and quantitatively its occurrence.

We will assume that the orbitals of the Slater determinant are simple plane waves through this whole section and generalize the results to any kind of orbitals in Sec. IV.

A. Ratio with a positive-definite distribution

The expectation value of an operator O computed averaging over a Shadow Wave Function is

$$\begin{aligned} \langle O \rangle &= \frac{\int dR dS_1 dS_2 \varphi_{\text{SWF}}^*(R, S_1) O \varphi_{\text{SWF}}(R, S_2)}{\int dR dS_1 dS_2 \varphi_{\text{SWF}}^*(R, S_1) \varphi_{\text{SWF}}(R, S_2)} \\ &= \frac{\int dR dS_1 dS_2 \varphi_{\text{SWF}}^*(R, S_1) \varphi_{\text{SWF}}(R, S_2) O_{\text{L}}(R, S_2)}{\int dR dS_1 dS_2 \varphi_{\text{SWF}}^*(R, S_1) \varphi_{\text{SWF}}(R, S_2)} \end{aligned} \quad (13)$$

where

$$O_{\text{L}}(R, S) \equiv \frac{O \varphi_{\text{SWF}}(R, S)}{\varphi_{\text{SWF}}(R, S)}. \quad (14)$$

If we denote by $\rho(R, S_1, S_2)$ the probability density function (pdf) that we intend to sample from, and introduce the corresponding weight

$$w(R, S_1, S_2) = \frac{\varphi_{\text{SWF}}^*(R, S_1) \varphi_{\text{SWF}}(R, S_2)}{\rho(R, S_1, S_2)}, \quad (15)$$

then we can recast Eq. (13) as

$$\langle O \rangle = \frac{\int dR dS_1 dS_2 \rho(R, S_1, S_2) w(R, S_1, S_2) O_{\text{L}}(R, S_2)}{\int dR dS_1 dS_2 \rho(R, S_1, S_2) w(R, S_1, S_2)}. \quad (16)$$

If the product $\varphi_{\text{SWF}}^*(R, S_1) \times \varphi_{\text{SWF}}(R, S_2)$ is positive-definite, it is then possible to set ρ such that $w = 1$ and no sign problem occurs.

However, if this is not the case, a typical choice is

$$\rho(R, S_1, S_2) \equiv |\varphi_{\text{SWF}}^*(R, S_1) \varphi_{\text{SWF}}(R, S_2)| \quad (17)$$

and therefore

$$w(R, S_1, S_2) = \text{sign}(\varphi_{\text{SWF}}^*(R, S_1) \varphi_{\text{SWF}}(R, S_2)) = \pm 1. \quad (18)$$

and a sign problem occurs. The expectation value of O is then

$$\langle O \rangle = \frac{\langle w O_L \rangle_\rho}{\langle w \rangle_\rho} \quad (19)$$

where by $\langle \dots \rangle_\rho$ we mean the average resulting from sampling the pdf ρ .

Let us now focus on $\langle w \rangle_\rho$.

In the case of PIGS with a projection time τ or Path-Integral Monte Carlo at finite temperature $T = 1/\tau$, $\langle w \rangle_\rho$ is equal to the ratio between the fermionic and the bosonic partition functions [33] (where the bosonic system is defined by the positive-definite weight $|w|$) and therefore

$$\langle w \rangle_\rho = e^{-\tau N \Delta F} \quad (20)$$

where N is the number of particles and ΔF is the free energy difference between the bosonic and the fermionic system. It is important to keep in mind that such a condition can be fulfilled also by a fermionic system, as it is the case for the ASWF in one spatial dimension. In any case, the relation (20) explains the exponential decay in efficiency, as

$$\frac{\sigma(\langle w \rangle_\rho)}{\langle w \rangle_\rho} = \sqrt{\frac{\langle w^2 \rangle_\rho - \langle w \rangle_\rho^2}{M \langle w \rangle_\rho^2}} = \sqrt{\frac{1/\langle w \rangle_\rho^2 - 1}{M}} \sim \frac{e^{\tau N \Delta F}}{\sqrt{M}} \quad (21)$$

where M is the number of sampled points. By noticing that the relative error of $\langle O \rangle$ is given by the sum of the relative error of $\langle w O_L \rangle_\rho$ plus the one of $\langle w \rangle_\rho$, we can see that Eq. (21) is sufficient to explain the exponential decay of the efficiency with N and τ .

In the case of the SWF, we can evaluate $\langle w \rangle_\rho$ explicitly, by making two assumptions:

- i The bosonic system is represented by an ASWF;
- ii Correlation factors (Jastrow) do not play a crucial role and therefore can be omitted.

In subsection III B we will obtain the same results without making use of such assumptions, better justifying their validity.

Summarizing up, we want to compute the $\langle w \rangle_\rho$ associated to Ψ_{FSWF} , sampling from the ASWF. In formula

$$\langle w \rangle_{\text{FSWF}} = \frac{\int dR dS_1 dS_2 \varphi_{\text{FSWF}}^*(R, S_1) \varphi_{\text{FSWF}}^*(R, S_2)}{\int dR dS_1 dS_2 \varphi_{\text{ASWF}}^*(R, S_1) \varphi_{\text{ASWF}}^*(R, S_2)} \quad (22)$$

with

$$\begin{aligned} \varphi_{\text{FSWF}}(R, S) &= e^{-C(R-S)^2} \det(e^{i\mathbf{k}_\alpha \cdot \mathbf{s}_\beta}) \\ \varphi_{\text{ASWF}}(R, S) &= e^{-C(R-S)^2} \det(e^{i\mathbf{k}_\alpha \cdot \mathbf{r}_\beta}). \end{aligned} \quad (23)$$

where exactly N wave vectors \mathbf{k} are occupied in the Slater determinant, and where we assume a spin-polarized system with N fermions for simplification. We then have

$$\begin{aligned} \int dS e^{-C(R-S)^2} \det(e^{i\mathbf{k}_\alpha \cdot \mathbf{s}_\beta}) &= \\ \left(\frac{\pi}{C}\right)^{\frac{3N}{2}} e^{-\frac{\sum_{i=1}^N \mathbf{k}_i^2}{4C}} \det(e^{i\mathbf{k}_\alpha \cdot \mathbf{r}_\beta}) \end{aligned} \quad (24)$$

so that we can integrate out $dS_1 dS_2$, and obtain

$$\begin{aligned} \langle w \rangle_{\text{FSWF}} &= \frac{e^{-\frac{\sum_{i=1}^N \mathbf{k}_i^2}{4C}} \int dR \det(e^{-i\mathbf{k}_\alpha \cdot \mathbf{r}_\beta}) \det(e^{i\mathbf{k}_\alpha \cdot \mathbf{r}_\beta})}{\int dR \det(e^{-i\mathbf{k}_\alpha \cdot \mathbf{r}_\beta}) \det(e^{i\mathbf{k}_\alpha \cdot \mathbf{r}_\beta})} \\ &= e^{-\frac{\sum_{i=1}^N \mathbf{k}_i^2}{4C}}. \end{aligned} \quad (25)$$

In the thermodynamic limit we get

$$\langle w \rangle_{\text{FSWF}} \propto e^{-\frac{N}{C} \rho^{2/3}}. \quad (26)$$

where ρ is the density. Then, the efficiency of a QMC simulation for computing $\langle O \rangle$ employing the FSWF writes

$$\eta \propto e^{-\frac{N}{C} \rho^{2/3}}. \quad (27)$$

B. Difference with a positive-definite distribution

In this subsection we will obtain the same result of the previous one, but without need of any special assumption.

In the spirit of the *control variates* technique [34, 35], we recast the FSWF as

$$\begin{aligned} \Psi_{\text{FSWF}}(R) &= \int dS (\varphi_{\text{FSWF}}(R, S) - \tilde{\varphi}_{\text{FSWF}}(R, S)) \\ &+ \int dS \tilde{\varphi}_{\text{FSWF}}(R, S), \end{aligned} \quad (28)$$

with the intention of eliding the first integral and let only the second one survive, which will be built in order to avoid the fermion sign problem.

With this aim in mind, we set

$$\tilde{\varphi}_{\text{FSWF}}(R, S) = J_{\text{R}}(R) \tilde{J}_{\text{S}}(R) \Xi(R, S) \Phi(S) \quad (29)$$

where $\tilde{J}_{\text{S}}(R)$ is a local normalization factor necessary to ensure that

$$\int dS \tilde{\varphi}_{\text{FSWF}}(R, S) = \int dS \varphi_{\text{FSWF}}(R, S) \quad (30)$$

In other words, $\tilde{\varphi}_{\text{FSWF}}$ is a fermionic shadow wave function in which the shadow-shadow correlation has been replaced by an effective local Jastrow $\tilde{J}_{\text{S}}(R)$. Although needed in our proof, the reader should bear in mind that such a normalization factor cannot be easily estimated, as its computation would fall in a sign problem.

We now integrate out the shadows, in order to eliminate the sign problem in the second integral of Eq. (28):

$$\begin{aligned} \bar{\Psi}_{\text{FSWF}}(R) &\equiv \int dS \tilde{\varphi}_{\text{FSWF}}(R, S) \\ &= J_{\text{R}}(R) \tilde{J}_{\text{S}}(R) \Phi(R) \left(\frac{\pi}{C}\right)^{\frac{3N}{2}} e^{-\frac{\sum_{i=1}^N \mathbf{k}_i^2}{4C}} \\ &= J_{\text{R}}(R) \tilde{J}_{\text{S}}(R) \Phi(R) e^{-\frac{\sum_{i=1}^N \mathbf{k}_i^2}{4C}} \int dS \Xi(R, S) \\ &= \int dS \bar{\varphi}_{\text{FSWF}}(R, S) \end{aligned} \quad (31)$$

where we have formally reintroduce the shadows. We can see that $\tilde{\Psi}_{\text{FSWF}}$ can be regarded as the closest ASWF to the given FSWF, i.e. a "bosonized" FSWF. Notice that $\tilde{\Psi}_{\text{FSWF}}(R)$ does not contain a Slater determinant evaluated on the shadow coordinates anymore, hence this wave function is not affected by the sign problem.

The FSWF can now be written as

$$\begin{aligned} \Psi_{\text{FSWF}}(R) &= \int dS [\varphi_{\text{FSWF}}(R, S) - \tilde{\varphi}_{\text{FSWF}}(R, S) \\ &\quad + \bar{\varphi}_{\text{FSWF}}(R, S)] \\ &= J_{\text{R}}(R) \int dS \Xi(R, S) \tilde{J}_{\text{S}}(R) \times \\ &\quad \left[\Phi(S) \left(\frac{J_{\text{S}}(S)}{\tilde{J}_{\text{S}}(R)} - 1 \right) + \Phi(R) e^{-\frac{\sum_{i=1}^N \mathbf{k}_i^2}{4C}} \right] \end{aligned} \quad (32)$$

If the term $\left(\frac{J_{\text{S}}(S)}{J_{\text{S}}(R)} - 1 \right)$ were zero, we would have solved the sign problem.

Let us now assume to be able to sample from the signal, i.e.

$$\rho(R, S_1, S_2) = \bar{\varphi}_{\text{FSWF}}^*(R, S_1) \bar{\varphi}_{\text{FSWF}}(R, S_2), \quad (33)$$

then the weight corresponding to our original sampling, Eq. (32), writes

$$\begin{aligned} w(R, S_1, S_2) &= \left[1 + \frac{\Phi(S_1)}{\Phi(R)} \left(\frac{J_{\text{S}}(S_1)}{\tilde{J}_{\text{S}}(R)} - 1 \right) e^{\frac{\sum_{i=1}^N \mathbf{k}_i^2}{4C}} \right] \\ &\quad \times \left[1 + \frac{\Phi(S_2)}{\Phi(R)} \left(\frac{J_{\text{S}}(S_2)}{\tilde{J}_{\text{S}}(R)} - 1 \right) e^{\frac{\sum_{i=1}^N \mathbf{k}_i^2}{4C}} \right] \end{aligned} \quad (34)$$

which can be seen as

$$\text{weight} = \text{signal} + \text{noise} \quad (35)$$

where signal = 1. Hence, we require that

$$|\langle \text{noise} \rangle| < |\langle \text{signal} \rangle| \quad (36)$$

or, by expanding,

$$\begin{aligned} &\left| \left\langle \frac{\Phi(S_1)}{\Phi(R)} \left(\frac{J_{\text{S}}(S_1)}{\tilde{J}_{\text{S}}(R)} - 1 \right) \right\rangle e^{\frac{\sum_{i=1}^N \mathbf{k}_i^2}{4C}} \right. \\ &+ \left. \left\langle \frac{\Phi(S_2)}{\Phi(R)} \left(\frac{J_{\text{S}}(S_2)}{\tilde{J}_{\text{S}}(R)} - 1 \right) \right\rangle e^{\frac{\sum_{i=1}^N \mathbf{k}_i^2}{4C}} \right. \\ &+ \left. \left\langle \frac{\Phi(S_1)\Phi(S_2)}{\Phi^2(R)} \left(\frac{J_{\text{S}}(S_1)}{\tilde{J}_{\text{S}}(R)} - 1 \right) \right. \right. \\ &\quad \left. \left. \times \left(\frac{J_{\text{S}}(S_2)}{\tilde{J}_{\text{S}}(R)} - 1 \right) \right\rangle e^{2\frac{\sum_{i=1}^N \mathbf{k}_i^2}{4C}} \right| < 1 \end{aligned} \quad (37)$$

Equation (37) is necessary condition to avoid the sign problem, and it contains all the informations that we are looking for.

In particular, we would like to know how the sign problem scales with the number of particles. We then use the

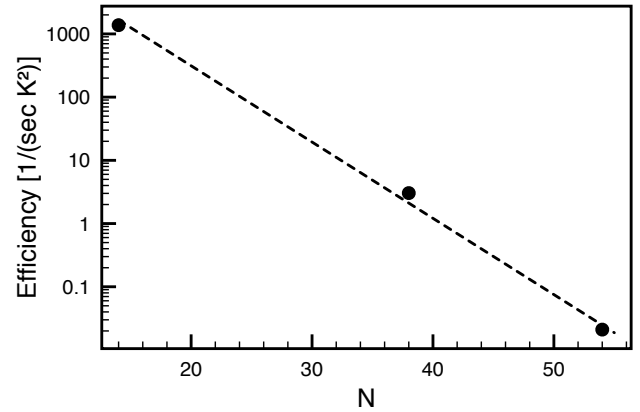


Figure 2. Efficiency of a VMC simulation of liquid ${}^3\text{He}$ that employs the FSWF [32], fitted with an exponential function $\sim e^{-kN}$, where k is a constant.

following reasoning: Suppose that we have performed a calculation with N_0 particles which provided us the estimate we were seeking for, with an agreeable error bar. We label the corresponding efficiency with η_0 . We then change the number of particles to $N = \kappa_N N_0$. It is now possible to tell how the fermion sign problem will affect the efficiency of the QMC simulation. In fact, suppose that we want to obtain a result with the same accuracy. We will then require that the noise in the weight will be the same, i.e. $\langle \text{noise} \rangle = \langle \text{noise}_0 \rangle$. From Eq. (37), we can read a dependence from the number of particles in the terms $e^{-\frac{\sum_{i=1}^N \mathbf{k}_i^2}{4C}} \simeq e^{-\frac{N}{C} \rho^{2/3}}$. Then, we need the averages in Eq. (37) to diminish by a factor $e^{-\kappa_N}$. We remark that we know that such averages will eventually be equal to zero, therefore to make them diminish it basically means to diminish their corresponding error bar. However, smaller error bars require longer sampling, which in turn implies longer simulation time. Assuming the variance of the noise integrand to be independent of N , we have $\sigma \propto (\text{number of sampled points})^{-1/2} \propto (\text{cpu time})^{-1/2}$ and we can conclude that $\log \eta / \eta_0 \propto -\kappa_N$. Similarly, we can derive the dependencies for C and ρ , which gives

$$\log \eta / \eta_0 \propto -\frac{N}{C} \rho^{2/3}. \quad (38)$$

We have derived the result of the previous subsection in a more general situation.

These prediction are confirmed by the numerical results reported in [32]. In Figures 2 and 3 the data are fitted with an exponential function, demonstrating the exponential dependency on N and C . Data refer to the computation of the total energy of the 3D unpolarized liquid ${}^3\text{He}$ ($\rho = 0.016588 \text{ \AA}^{-3}$) by means of VMC, employing the FSWF as trial wave function.

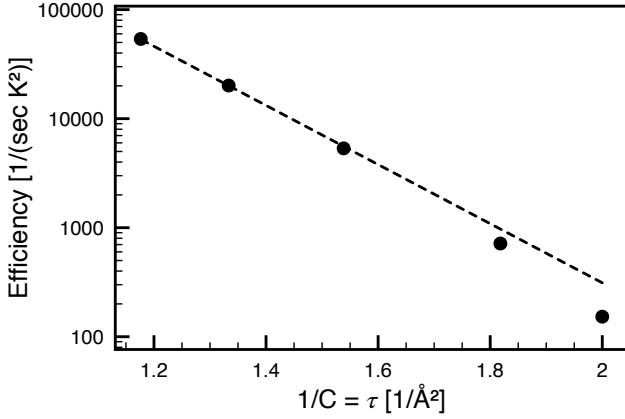


Figure 3. Efficiency of a VMC simulation of liquid ^3He that employs the FSWF [32], fitted with an exponential function $\sim e^{-k/C}$, where k is a constant.

IV. GENERALIZATION TO ANY KIND OF ORBITALS

In this section we are going to generalize the dependence of the efficiency on N , C , and ρ to the more general case of Slater determinants which use any kind of orbitals.

To accomplish this result it is sufficient to work in the Fourier space. The matrix elements of the Slated determinant can be expressed as an integral over the N -particle momentum space of a product of matrices:

$$\begin{aligned} \phi_\alpha(\mathbf{r}_\beta) &= \int d\mathbf{k}_\alpha e^{-i\mathbf{k}_\alpha \cdot \mathbf{r}_\beta} \tilde{\phi}_\alpha(\mathbf{k}_\alpha) \\ &= \int dK \sum_{\gamma=1}^N (e^{-i\mathbf{k}_\gamma \cdot \mathbf{r}_\beta}) (\tilde{\phi}_\alpha(\mathbf{k}_\gamma) \delta_{\gamma\alpha}) \\ &= \int dK (e^{-i\mathbf{k}_\gamma \cdot \mathbf{r}_\beta}) \cdot (I_{\tilde{\phi}_\alpha(\mathbf{k}_\gamma)}), \end{aligned} \quad (39)$$

where $\tilde{\phi}(\mathbf{k})$ is the Fourier transform of the orbital $\phi(\mathbf{r})$, and

$$I_{\tilde{\phi}_\alpha(\mathbf{k}_\gamma)} \equiv \tilde{\phi}_\alpha(\mathbf{k}_\gamma) \delta_{\gamma\alpha}.$$

Therefore

$$\begin{aligned} \det(\phi_\alpha(\mathbf{r}_\beta)) &= \int dK \det(e^{-i\mathbf{k}_\gamma \cdot \mathbf{r}_\beta}) \det(I_{\tilde{\phi}_\alpha(\mathbf{k}_\gamma)}) \\ &= \int dK \det(e^{-i\mathbf{k}_\gamma \cdot \mathbf{r}_\beta}) \prod_{\gamma=1}^N \tilde{\phi}_\gamma(\mathbf{k}_\gamma) \end{aligned} \quad (40)$$

In the following we will use the notation

$$\begin{aligned} \Phi(R) &\equiv \det(\phi_\alpha(\mathbf{r}_\beta)) \\ \tilde{\Phi}(K) &\equiv \prod_{\gamma=1}^N \tilde{\phi}_\gamma(\mathbf{k}_\gamma) \end{aligned} \quad (41)$$

and

$$\Phi_{\text{pw}}(R, K) \equiv \det(e^{-i\mathbf{k}_\alpha \cdot \mathbf{r}_\beta}) \quad (42)$$

Following the idea used in subsection III B, we write:

$$\begin{aligned} \varphi_{\text{FSWF}}(R, S, K) &= J_R(R) \Xi(R, S) J_S(S) \tilde{\Phi}(K) \Phi_{\text{pw}}(R, S) \\ \tilde{\varphi}_{\text{FSWF}}(R, S, K) &= J_R(R) \tilde{J}_S(R) \Xi(R, S) \tilde{\Phi}(K) \Phi_{\text{pw}}(R, S) \\ \bar{\varphi}_{\text{FSWF}}(R, S, K) &= J_R(R) \tilde{J}_S(R) \Xi(R, S) e^{-\frac{\sum_{i=1}^N \mathbf{k}_i^2}{4C}} \\ &\quad \times \tilde{\Phi}(K) \Phi_{\text{pw}}(R, K). \end{aligned} \quad (43)$$

Eq. (32) can be then recast as

$$\begin{aligned} \Psi_{\text{FSWF}}(R) &= J_R(R) \int dS dK \Xi(R, S) \tilde{J}_S(R) \times \\ &\quad \left[\tilde{\Phi}(K) \Phi_{\text{pw}}(S) \left(\frac{J_S(S)}{\tilde{J}_S(R)} - 1 \right) \right. \\ &\quad \left. + \tilde{\Phi}(K) \Phi_{\text{pw}}(R) e^{-\frac{\sum_{i=1}^N \mathbf{k}_i^2}{4C}} \right], \end{aligned} \quad (44)$$

while Eq. (37) will now read

$$\begin{aligned} &\left| \left\langle \frac{\Phi_{\text{pw}}(S_1, K_1)}{\Phi_{\text{pw}}(R, K_1)} \left(\frac{J_S(S_1)}{\tilde{J}_S(R)} - 1 \right) e^{\frac{\sum_{i=1}^N \mathbf{k}_i^2}{4C}} \right\rangle \right. \\ &+ \left. \left\langle \frac{\Phi_{\text{pw}}(S_2, K_2)}{\Phi_{\text{pw}}(R, K_2)} \left(\frac{J_S(S_2)}{\tilde{J}_S(R)} - 1 \right) e^{\frac{\sum_{i=1}^N \mathbf{k}_i^2}{4C}} \right\rangle \right. \\ &+ \left. \left\langle \frac{\Phi_{\text{pw}}(S_1, K_1) \Phi_{\text{pw}}(S_2, K_2)}{\Phi_{\text{pw}}(R, K_1) \Phi_{\text{pw}}(R, K_2)} \left(\frac{J_S(S_1)}{\tilde{J}_S(R)} - 1 \right) \right. \right. \\ &\quad \left. \left. \times \left(\frac{J_S(S_2)}{\tilde{J}_S(R)} - 1 \right) e^{2\frac{\sum_{i=1}^N \mathbf{k}_i^2}{4C}} \right\rangle \right| < 1. \end{aligned} \quad (45)$$

By carefully inspecting Eq. (45) we notice that the role played by $e^{\frac{\sum_{i=1}^N \mathbf{k}_i^2}{4C}}$ is now played by

$$\left\langle \frac{\Phi_{\text{pw}}(S, K)}{\Phi_{\text{pw}}(R, K)} e^{\frac{\sum_{i=1}^N \mathbf{k}_i^2}{4C}} \right\rangle_K \quad (46)$$

where by $\langle \dots \rangle_K$ we mean the average over K obtained by sampling from $\bar{\varphi}_{\text{FSWF}}^*(R, S_1, K_1) \times \bar{\varphi}_{\text{FSWF}}(R, S_2, K_2)$ for any given R and S . In other words, the factor which control the efficiency of the calculation is now a function of R and S .

Since we have no simple interpretation of Eq. (46), we have numerically estimated its dependence on the degree of localization of the orbitals employed in the Slater determinant. For doing so we have neglected the Jastrow terms, and considered only a kernel Ξ and a Slater determinant Φ containing gaussian orbitals of the form $e^{-G(S-P)^2}$, where P labels some lattice positions. Fig. 4 shows our results.

The numerical results demonstrate that the efficiency increases exponentially when the orbitals become more localized until it reaches a maximum and finally begins

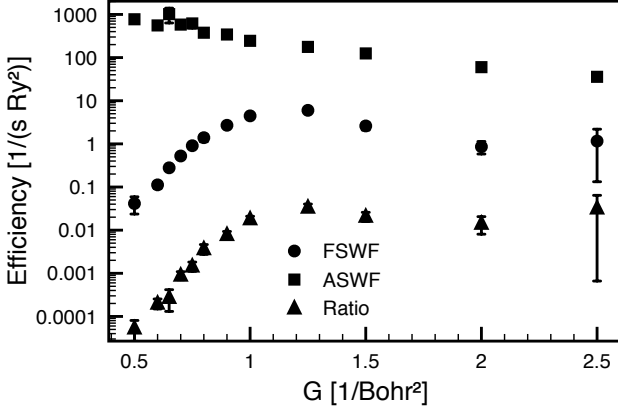


Figure 4. Efficiency as a function of the gaussian coefficient G which enters in the Slater determinant orbitals. The dataset Ratio reports the ratio between the FSWF and the ASWF values and therefore it is dimensionless. Results were obtained by computing the expectation value of the energy per particle of the electronic structure of an hydrogen bcc atomic crystal with $r_s = 1.7$ and periodic boundary conditions. The lattice positions required by the gaussians are the hydrogen's protons. We have used $C = 1$.

to decrease. Such decrease at large G is due to other reason than the sign problem, as it affects also the ASWF. Therefore, in order to isolate the sign problem dependency, we have introduced the ratio between the FSWF efficiency and the ASWF one, which are represented by triangular symbols in Fig. 4. Looking at these data, we can notice that at large G there is a plateau rather than a decay.

The threshold at which the ratio reaches a plateau can be interpreted as the degree of localization at which the fermionic statistic become irrelevant and the quantum particles can be conveniently approximated as distinguishable.

In conclusion we see that there is a strong dependence between the localization of the Slater determinant orbitals and the sign problem, with the latter one becoming more severe as the first one decreases.

V. ALLEVIATION OF THE FERMION SIGN PROBLEM AND APPROXIMATED METHODS

As we have shown in the previous Sections, the Fermi statistic entails a sign problem which in general makes simulations of large number of fermions prohibitive. Nevertheless, given the importance of fermionic systems for the comprehension of many natural phenomena (e.g. quantum chemistry), many methods which cope with such difficulties have been devised and are used on a daily routine. Here we will focus on the methods which involve the Monte Carlo algorithms.

A first naive approach is to try to keep τ as small as possible, and employ a very good starting trial function.

In this way, it is possible to find a lower upper bound to the exact ground state energy, systematically improvable by increasing the quality of the trial function. This approach goes under the name of *release-node* or *transient estimates* [18, 19, 36–39], and it corresponds to the naive employment of the FSWF with a value of C as small as possible within given computational limits. Such methods would greatly benefit from any method able to alleviate the severity of the sign problem. In the past years some remarkable improvements have been achieved in this direction.

We begin by outlining briefly the *Gaussian Determinant* (G_{\det}) method [29], introduced for the study of vacancies in solid ^3He , and further investigated in [32]. The leading idea is to sum over all the possible shadow permutations by means of an anti-symmetrical kernel consisting of a determinant of gaussian orbitals. In practice, it is sufficient to replace the kernel with

$$\Xi(R, S) \rightarrow G_{\det}(R, S) \equiv \det \left(e^{-C(\mathbf{r}_\alpha - \mathbf{s}_\beta)^2} \right), \quad (47)$$

where α and β label a matrix row and column. Fig. 5 and 6 demonstrate that the exponential pre-factor is significantly reduced. The extension of the G_{\det} technique to PIGS is straightforward, as it is sufficient to replace each gaussian kernel with a determinant of gaussians, exactly as for the SWF. In the (unconstrained-node) DMC method instead, one has to make the walkers diffuse according to the standard gaussian term, and then multiply the branching by

$$G_{\det}(R, R') / \exp \left(-\frac{(R - R')^2}{4\tau} \right), \quad (48)$$

which will typically be positive and very close to 1, as in DMC τ needs to be very small. A negative value of G_{\det} would imply a switch of the walker from the population carrying a positive sign to the one representing the negative contribution.

A second method which have been devised in recent time and have shown positive results is the *Approximated Marginal Distribution Method* (AMD) [32]. Here, the leading idea is to sample the R coordinates from a modified sampling distribution which is intended to account for the integration over the shadows, and therefore provides a better representation of the marginal distribution for R . At the same time, the weights which carry the sign are computed by summing up the contributions coming from multiple sampling of the shadows, according to the grouping technique. The improvements attainable with this method can be seen in Fig. 7 and 8. We point out that this method is valuable when the sign problem is "strong", whereas the naive algorithms outperforms it in the other situations.

Whereas other general methods proven to alleviate the fermion sign problem without approximation are not known to the best of our knowledge, several approximated techniques which avoid the sign problem are used

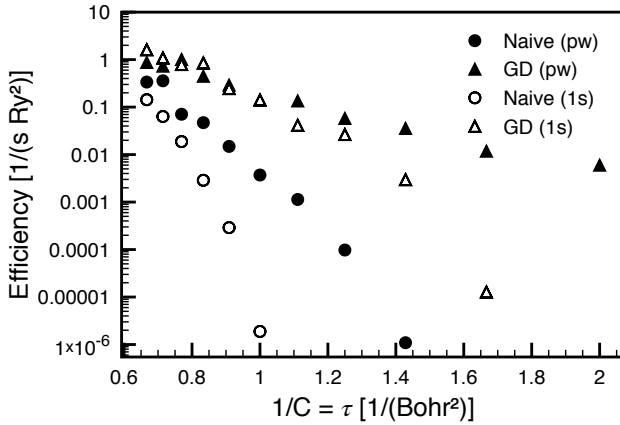


Figure 5. Comparison between a naive simulation employing the FSWF and a calculation which employs the G_{det} formulation. The efficiency is calculated for different C and with two different choices for the orbitals embedded in the Slater determinant: The 1s orbitals and simple plane-waves (pw). To obtain these results we simulated the electronic structure of 3D solid hydrogen with a bcc crystal structure and $r_s = 1.8$, employing a Yukawa Jastrow both for J_R and J_S . The results refer to simulations done with 16 atoms.

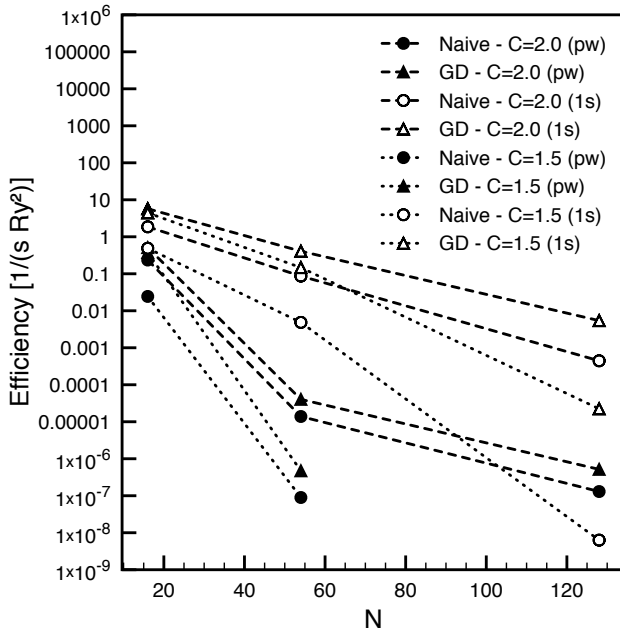


Figure 6. Same as in Fig. 5 but exploring the efficiency dependency on N . We show the results for different orbitals and choices of C . The simulated physical system was the same as for Fig. 5.

routinely. Probably the most re-known one is the fixed-node approximation [36, 37, 41–43] which imposes a nodal surface, forcing the solution to be antisymmetrical. Concretely, this is accomplished by taking an antisymmetrical wave function φ_T and use the DMC scheme restricted to the positive (or negative) domain of φ_T :

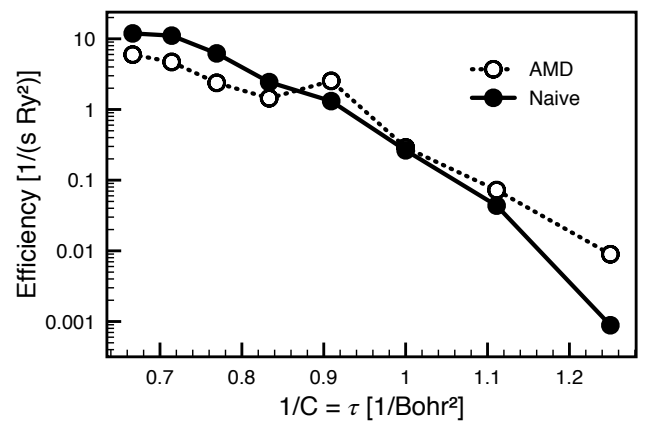


Figure 7. Performance comparison between calculations with the FSWF using the naive algorithm and the AMD method, for different values of C . The results refer to the computation of the potential energy of the electronic structure of 16 hydrogen atoms in a bcc crystal structure at $r_s = 1.8$. We employed a Yukawa Jastrow both for J_R and J_S , and 1s orbitals within the Slater determinant. For approximating the marginal distribution, we used a Slater determinant embedding orbitals found by using Quantum Espresso [40]. The AMD results refer to the best efficiency attainable by varying the parameters Λ and M_S (see [32]).

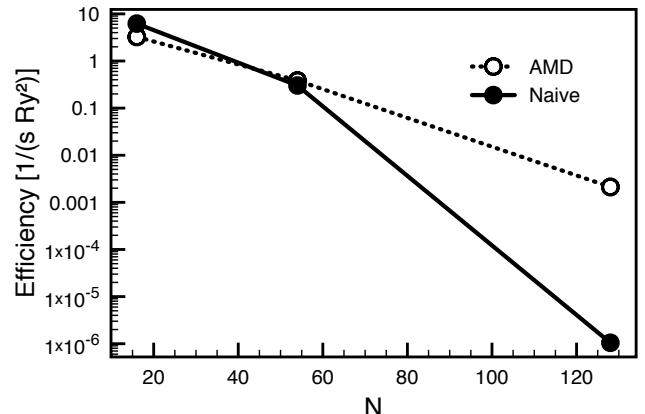


Figure 8. Same as in Fig. 7 but changing the number of simulated particles N . We used $C = 1.3 \text{ Bohr}^{-2}$.

Whenever a walker crosses the nodal surface, it is suppressed. Through this procedure it is possible to filter the best antisymmetrical ground state with the given nodal surface. Therefore, the nodal surface is the input that will determine the quality of the final result. The fixed-node approximation has been successfully extended to Path Integral Monte Carlo [44]. For transferring the fixed-node method to FSWF calculations, it is sufficient to choose a nodal surface (typically using the Slater determinant of the FSWF) and require that S and its imaginary time projection R are in the same nodal region.

In the following we outline three general approaches

which have been devised in the past and aimed to an exact solution of the fermion sign problem. Even if they have not been able to beat its exponential behaviour, they might have the potential to alleviate this trend. Unfortunately there are not data available, therefore we are not able to tell if this is the case.

In 1982, a Green's function Monte Carlo algorithm for fermions based on a *cancellation process* has been introduced [45]. The proposed algorithm is based on the intuitive idea of having two different populations of walker, one carrying a positive sign, and the other one a negative sign, which will cancel each other if they get "close enough". The method has been employed for few particle systems, but it suffers from a substantial drawback that prevents its application to many-body system. The reason behind this is that the algorithm requires a high density of walkers, and unfortunately such requirement implies an exponential growth of the computational cost proportional to the number of simulated particles, because of the increased dimensionality of the problem. Further works in the same direction [20, 21, 46, 47] have not been able to solve the fermion sign problem.

In 1985 a method for treating the fermion sign problem involving *mirror potentials* has been devised [39], where a fictitious repulsive interaction is used to keep the distribution of positive and negative walkers apart from each other, and hence avoid the collapse into the same bosonic ground state. By increasing the repulsion between the two populations this method reduces to the fixed-node approximation, whereas when it is set to zero one obtains a release-node simulation. The mirror potential method allows exact fermion calculations, but is limited to a small number of particles due to the exponential growth in number of walkers required to describe the mirror potential, similarly to what happened with the cancellation idea. To overcome the over-mentioned difficulty, it is possible to make use of a trial wave function. However this will lead to an approximate result, although potentially more accurate than the fixed-node one.

In the context of Path Integral Monte Carlo, there has been an interesting attempt toward the solution of the fermion sign problem in 1998-2000 [48, 49]. The proposed approach goes under the name of *multilevel blocking*, and it consists into distributing the integrals for the propagation of a single imaginary time step $\Delta\tau$ in an elaborated pyramidal structure, and solving it in a bottom-up fashion. First one computes the $N_\tau/2$ integrals at the bottom, and then use these informations to compute the integrals at a coarser level, i.e. for $2\Delta\tau$. This procedure is repeated until the integral for the full imaginary-time propagation $N_\tau\Delta\tau$ is found. However, we have seen that even a single integration step already introduces a sign problem which scales exponentially in the number of particles, so that the proposed scheme will eventually scale exponentially, too.

In 2009 a new method (FCIQMC) for treating fermion very accurately [50] has been introduced, based on a

Monte Carlo imaginary-time projection technique performed in a space of Slater determinants, in the spirit of Full Configuration Interaction (FCI). In this method, if the number of walkers is sufficient to populate such space, the FCI wave function will emerge from the calculation within a less severe computational cost compared to the traditional schemes, as a result of the Monte Carlo methods suitability in handling high dimensionality [51]. However, the use of such variational space for treating particle correlation imply a size-extensivity problem. Nevertheless, this method has demonstrated to be competitive with other highly-accurate methods employed in quantum chemistry [52–56].

VI. COMPUTATIONAL COMPLEXITY OF THE FERMION SIGN PROBLEM

This section is dedicated to discuss the computational complexity of the fermion sign problem in QMC. Before going into the details, we would like to briefly introduce the reader to the complexity classes P, NP, NPC, and NP-hard. The interested reader can refer to [8, 57, 58] for an exhaustive introduction to the topic.

P is the class of problems which are solvable in polynomial time: Provided an input problem of size n , it exists an algorithm which can solve it in $O(n^k)$ time (here we are making use of the big O notation), where k is a constant. In our specific case, the input is provided by the physical parameters of the system, the variational parameters to be employed, and the Hamiltonian of the system. The problem's size is given by the number of simulated particles.

NP (Nondeterministic Polynomial) problems are the ones which can be verified in polynomial time: Given a solution (*certificate*) of the problem, it exists an algorithm that can verify its correctness in $O(n^k)$ time. We remark that any problem in P belongs also to NP, because if it is possible to solve a problem in polynomial time, such a solution can be used to verify a certificate.

In order to illustrate the NPC and the NP-hard classes we need to further introduce the concept of *reducibility*. The problem A is said to be *polynomial-time reducible* to problem B if it is possible to find a map $A \mapsto B$ which is computable in polynomial time.

The NPC (*NP-Complete*) problems are the NP problems which have the additional property of being polynomial-time reducible to any other NP problem. If a problem possesses the latter property but not necessarily the first one, then it is said to be *NP-hard*.

In the work of Troyer and Wiese [9], it has been shown that a general QMC algorithm which is able to compute the most general partition function can also be used to solve a NPC problem. The reference NPC problem [59] is the following: Given a classical 3D Ising spin glass with Hamiltonian

$$H = - \sum_{\langle i_1, i_2 \rangle} J_{i_1 i_2} S_{i_1} S_{i_2} \quad (49)$$

and a bound energy E_0 , does a spin configuration with energy $E \leq E_0$ exist? The interaction matrix J has values j , 0, or $-j$ chosen randomly, and the spins S can have values ± 1 .

The latter decision problem is connected to Monte Carlo calculations by the fact that provided a large enough inverse temperature β , the average energy of the spin glass system will be less than $E_0 + j/2$ if a configuration with $E \leq E_0$ exists, and larger than $E_0 + j$ otherwise (basically, the simulated annealing minimization method). As a consequence, the computation of E with a Monte Carlo simulation would provide an answer to the given 3D Ising spin glass NPC problem. In other words, such Monte Carlo average is necessarily at least as hard as a NPC problem, i.e. it is NP-hard.

Since the classical NPC problem in Eq. (49) can be mapped in a quantum one simply by replacing classical spins with quantum ones, a general algorithm to solve quantum problems (including those with a sign problem) will provide also a solution to our NPC problem and thus will be NP-hard [9]. However, not all many-fermion systems pose NP hard problems and it remains open if there is a criterion that allows us to immediately distinguish a NP-hard simulation from a P one (or, strictly speaking, Bounded-error Probability Polynomial).

It would be of great importance to be able to better characterise the fermion sign problem complexity. Is it possible to devise a criterion in order to predict when the QMC simulation will be NP-hard? Is it possible to find a case in which the NP-hardness originate from the fermion statistic? Some progresses in this direction have been done recently [60] identifying sets of Hamiltonians without sign problem.

In the following we discuss a definition of the fermion sign problem concerning purely continuum QMC simulation with local interactions, using the SWF formalism.

Decisional fermion sign problem: Is the value of the integral

$$\int dS e^{-C(R-S)^2} \det(\phi_\alpha(\mathbf{s}_\beta)) J_s(S) \quad (50)$$

strictly greater than zero?

If one could answer to this decisional problem, exact fermion calculations in polynomial time would be possible by employing the fixed-node algorithm. If the provided answer is affected by a statistical error, as it would be the case by using a Monte Carlo technique, then the fixed-node method will have to make use of the penalty method [61], whose efficiency will decrease exponentially with the given statistical error.

Notice that this decisional problem does not admit the existence of a certificate, as it is not in the form "does ... such that ... exists?". Therefore one should find a corresponding problem which will allow to identify it as a NP-hard problem (if it is such). We leave this question open.

VII. CONCLUSION

We have presented the SWF formalism and showed that the fermion sign problem appearing in typical imaginary-time projection continuum QMC methods can be reduced to the sign problem of the Fermionic Shadow Wave Function. This formalism was used to characterise both analytically and numerically the fermion sign problem, demonstrating its dependence on the number of particles, length of the imaginary-time projection, and localisation of the system. Even though it seems that the exponential decay of the simulation efficiency cannot be overcome, we have shown that some methods can lead to a significative reduction of its exponential factor, thus extending the applicability of exact QMC methods for fermions. Concerning the complexity class of imaginary-time projection QMC algorithms, a separate proof of the NP-hardness of 2D and 3D fermionic systems with local interactions in continuum space is still lacking.

ACKNOWLEDGMENTS

F.C. would like to acknowledge the Nanosciences Foundation of Grenoble for financial support and T. D. Kühne for allowing access to the Mogon HPC which has been used for most of the numerical calculations.

[1] J. E. Hirsch and R. M. R Martin Fye, Phys. Rev. Lett. **56**, 2521 (1986).

[2] P. Broecker and S. Trebst, Cond-Mat, arXiv:1511.02878 (2015).

[3] L. Wang, Y.-H. Liu, M. Iazzi, M. Troyer, and G. Harcos, Cond-Mat, arXiv:1506.05349 (2015).

[4] M. A. Morales, R. Clay, C. Pierleoni, and D. M. Ceperley, Entropy **16**, 287 (2014).

[5] B. M. Austin, D. Y. Zubarev, and W. A. Lester, Chem. Rev. **112**, 263 (2012).

[6] J. Kolorenc and L. Mitas, Rep. Prog. Phys. **74**, 026502 (2011).

[7] R. J. Needs, M. D. Towler, N. D. Drummond, and P. L. Rios, J. Phys.: Condens. Matter **22**, 023201 (2010).

[8] T. H. Cormen, C. E. Leiserson, R. L. Rivest, and C. Stein, *Introduction to Algorithms* (The MIT Press, 2009), 3rd ed.

[9] M. Troyer and U.-J. Wiese, Phys. Rev. Lett. **94**, 170201 (2005), URL <http://link.aps.org/doi/10.1103/PhysRevLett.94.170201>.

[10] S. Vitiello, K. Runge, and M. H. Kalos, Phys. Rev. Lett. **60**, 1970 (1988).

[11] L. Reatto and G. L. Masserini, Phys. Rev. B **38**, 4516 (1988).

[12] G. Laporte, European Journal of Operational Research **59**, 231 (1992), ISSN 0377-2217, URL <http://www.sciencedirect.com/science/article/pii/037722179290138Y>.

[13] B. Golden, L. Bodin, T. Doyle, and J. W. Stewart, Operations Research **28**, 694 (1980), URL <http://dx.doi.org/10.1287/opre.28.3.694>, URL <http://dx.doi.org/10.1287/opre.28.3.694>.

[14] C. J. Umrigar, J. Toulouse, C. Filippi, S. Sorella, and R. G. Hennig, Phys. Rev. Lett. **98**, 110201 (2007), URL <http://link.aps.org/doi/10.1103/PhysRevLett.98.110201>.

[15] M. Holzmann, B. Bernu, and D. M. Ceperley, Phys. Rev. B **74**, 104510 (2006).

[16] M. Taddei, M. Ruggeri, S. Moroni, and M. Holzmann, Phys. Rev. B **91**, 115106 (2015), URL <http://link.aps.org/doi/10.1103/PhysRevB.91.115106>.

[17] A. Lüchow and R. F. Fink, The Journal of Chemical Physics **113**, 8457 (2000), URL <http://scitation.aip.org/content/aip/journal/jcp/113/19/10.1063/1.1318748>.

[18] D. Ceperley and B. Alder, J. Chem. Phys. **81**, 5833 (1984).

[19] N. M. Tubman, J. L. DuBois, R. Q. Hood, and B. J. Alder, The Journal of Chemical Physics **135**, 184109 (2011), URL <http://scitation.aip.org/content/aip/journal/jcp/135/18/10.1063/1.3659143>.

[20] Z. Liu, S. Zhang, and M. H. Kalos, Phys. Rev. E **50**, 3220 (1994), URL <http://link.aps.org/doi/10.1103/PhysRevE.50.3220>.

[21] M. H. Kalos and F. Pederiva, Phys. Rev. Lett. **85**, 3547 (2000), URL <http://link.aps.org/doi/10.1103/PhysRevLett.85.3547>.

[22] C. Wu and S.-C. Zhang, Phys. Rev. B **71**, 155115 (2005), URL <http://link.aps.org/doi/10.1103/PhysRevB.71.155115>.

[23] C. Wu, J.-p. Hu, and S.-c. Zhang, Phys. Rev. Lett. **91**, 186402 (2003), URL <http://link.aps.org/doi/10.1103/PhysRevLett.91.186402>.

[24] G. Carleo, S. Moroni, F. Becca, and B. S., Phys. Rev. B **83**, 060411(R) (2011).

[25] M. Nava, A. Motta, D. Galli, E. Vitali, and S. Moroni, Phys. Rev. B **85**, 1184401 (2012).

[26] F. Pederiva, A. Ferrante, S. Fantoni, and L. Reatto, Phys. Rev. Lett. **72**, 2589 (1994).

[27] F. Pederiva, G. V. Chester, S. Fantoni, and L. Reatto, Phys. Rev. B **56**, 5909 (1997).

[28] F. Operetto and F. Pederiva, Phys. Rev. B **69**, 024203 (2004).

[29] L. Dandrea, F. Pederiva, S. Gandolfi, and M. H. Kalos, Phys. Rev. Lett. **102**, 255302 (2009), URL <http://link.aps.org/doi/10.1103/PhysRevLett.102.255302>.

[30] M. H. Kalos and L. Reatto, in *Progress in Computational Physics of Matter*, edited by L. Reatto and F. Manghi (World Scientific, Singapore, 1995).

[31] F. Calcavecchia and T. D. Kühne, EPL (Europhysics Letters) **110**, 20011 (2015), URL <http://stacks.iop.org/0295-5075/110/i=2/a=20011>.

[32] F. Calcavecchia, F. Pederiva, M. H. Kalos, and T. D. Kühne, Phys. Rev. E **90**, 053304 (2014), URL <http://link.aps.org/doi/10.1103/PhysRevE.90.053304>.

[33] D. M. Ceperley, in *Monte Carlo and Molecular Dynamics of Condensed Matter Systems*, edited by K. Binder and G. Ciccotti (Editrice Compositori, 1996), Studies in Classification, Data Analysis, and Knowledge Organization.

[34] H. Kahn and A. W. Marshall, Journal of the Operations Research Society of America **1**, 263 (1953), URL <http://pubsonline.informs.org/doi/pdf/10.1287/opre.1.5.263>, URL <http://pubsonline.informs.org/doi/abs/10.1287/opre.1.5.263>.

[35] M. H. Kalos and P. A. Whitlock, *Monte Carlo Methods* (Wiley-VCH, Weinheim, 2008).

[36] D. M. Ceperley and B. J. Alder, Phys. Rev. Lett. **45**, 566 (1980), URL <http://link.aps.org/doi/10.1103/PhysRevLett.45.566>.

[37] D. Ceperley and B. Alder, Science **231**, 555 (1986), URL <http://www.sciencemag.org/content/231/4738/555.full.pdf>, URL <http://www.sciencemag.org/content/231/4738/555.abstract>.

[38] M. A. Lee, K. E. Schmidt, M. H. Kalos, and G. V. Chester, Phys. Rev. Lett. **46**, 728 (1981), URL <http://link.aps.org/doi/10.1103/PhysRevLett.46.728>.

[39] J. Carlson and M. H. Kalos, Phys. Rev. C **32**, 1735 (1985), URL <http://link.aps.org/doi/10.1103/PhysRevC.32.1735>.

[40] P. Giannozzi, S. Baroni, N. Bonini, M. Calandra, R. Car, C. Cavazzoni, D. Ceresoli, G. L. Chiarotti, M. Cococcioni, I. Dabo, et al., Journal of Physics: Condensed Matter **21**, 395502 (19pp) (2009), URL <http://www.quantum-espresso.org>.

[41] P. Reynolds, D. Ceperley, B. Alder, and W. Lester Jr., J. Chem. Phys. **77**, 5593 (1982).

[42] J. B. Anderson, The Journal of Chemical Physics **63**, 1499 (1975), URL <http://scitation.aip.org/content/aip/journal/jcp/63/4/10.1063/1.431514>.

[43] J. W. Moskowitz, K. E. Schmidt, M. A. Lee, and M. H. Kalos, The Journal of Chemical Physics **77**, 349 (1982), URL <http://scitation.aip.org/content/aip/journal/jcp/77/1/10.1063/1.443612>.

[44] D. M. Ceperley, Phys. Rev. Lett. **69**, 331 (1992), URL <http://link.aps.org/doi/10.1103/PhysRevLett.69.331>.

[45] D. M. Arnow, M. H. Kalos, M. A. Lee, and K. E. Schmidt, The Journal of Chemical Physics **77**, 5562 (1982), URL <http://scitation.aip.org/content/aip/journal/jcp/77/11/10.1063/1.443762>.

[46] S. Zhang and M. H. Kalos, Phys. Rev. Lett. **67**, 3074 (1991), URL <http://link.aps.org/doi/10.1103/PhysRevLett.67.3074>.

[47] F. Pederiva and M. Kalos, Computer Physics Communications **121–122**, 440 (1999), ISSN 0010-4655, proceedings of the Europhysics Conference on Computational Physics {CCP} 1998, URL <http://www.sciencedirect.com/science/article/pii/S0010465599003781>.

[48] C. H. Mak, R. Egger, and H. Weber-Gottschick, Phys. Rev. Lett. **81**, 4533 (1998), URL <http://link.aps.org/doi/10.1103/PhysRevLett.81.4533>.

[49] R. Egger, L. Mühlbacher, and C. H. Mak, Phys. Rev. E **61**, 5961 (2000), URL <http://link.aps.org/doi/10.1103/PhysRevE.61.5961>.

[50] G. H. Booth, A. J. W. Thom, and A. Alavi, The Journal of Chemical Physics **131**, 054106 (2009), URL <http://scitation.aip.org/content/aip/journal/jcp/131/5/10.1063/1.3193710>.

[51] M. H. Kolodrubetz, J. S. Spencer, B. K. Clark, and W. M. C. Foulkes, J. Chem. Phys. **138**, 024110 (2013).

[52] D. M. Cleland, G. H. Booth, and A. Alavi, The Journal of Chemical Physics **134**, 024112

(2011), URL <http://scitation.aip.org/content/aip/journal/jcp/134/2/10.1063/1.3525712>.

[53] J. J. Shepherd, A. Grüneis, G. H. Booth, G. Kresse, and A. Alavi, Phys. Rev. B **86**, 035111 (2012), URL <http://link.aps.org/doi/10.1103/PhysRevB.86.035111>.

[54] G. H. Booth and A. Alavi, The Journal of Chemical Physics **132**, 174104 (2010), URL <http://scitation.aip.org/content/aip/journal/jcp/132/17/10.1063/1.3407895>.

[55] J. J. Shepherd, G. Booth, A. Grüneis, and A. Alavi, Phys. Rev. B **85**, 081103 (2012), URL <http://link.aps.org/doi/10.1103/PhysRevB.85.081103>.

[56] G. H. Booth, A. Gruneis, G. Kresse, and A. Alavi, Nature **493**, 0028 (2013), URL <http://dx.doi.org/10.1038/nature11770>.

[57] A. V. Aho and J. E. Hopcroft, *Design & Analysis of Computer Algorithms* (Pearson Education India, 1974).

[58] M. R. Garey and D. S. Johnson, San Francisco, LA: Freeman (1979).

[59] F. Barahona, Journal of Physics A: Mathematical and General **15**, 3241 (1982), URL <http://stacks.iop.org/0305-4470/15/i=10/a=028>.

[60] L. Wang, Y.-H. Liu, M. Iazzi, M. Troyer, and G. Harcos, ArXiv e-prints (2015), 1506.05349.

[61] D. M. Ceperley and M. Delsing, The Journal of Chemical Physics **110**, 9812 (1999), URL <http://scitation.aip.org/content/aip/journal/jcp/110/20/10.1063/1.478034>.